Journal of Organometallic Chemistry, 439 (1992) 221–230
Elsevier Sequoia S.A., Lausanne
JOM 22871

Characterization of 1 : 1 heterobimetallic complexes of (η^5-C_5Me_5)Ir(CO)$_2$ with zinc, cadmium and mercury(II) chloride and the X-ray structure determination of the 1 : 2 mercury complex

Frederick W.B. Einstein, Xiaoqian Yan, Xiaoheng Zhang and Derek Sutton
Department of Chemistry, Simon Fraser University, Burnaby, British Columbia V5A 1S6 (Canada)

(Received January 24, 1992)

Abstract

(η^5-C_5Me_5)Ir(CO)$_2$ reacts with $ZnCl_2$, $CdCl_2$ or $HgCl_2$ to produce the heterobimetallic complexes (η^5-C_5Me_5)(CO)$_2$IrMCl$_2$ (M = Zn (**1**), Cd (**2**), Hg (**3a**)) and [(η^5-C_5Me_5)(CO)$_2$IrHgCl][HgCl$_3$] (**3b**). The X-ray crystal structure of **3b** shows that the iridium atom adopts a three-legged piano stool coordination geometry, with two terminal CO ligands and an unbridged nearly linear, Ir–Hg–Cl group (Ir–Hg(1) = 2.587(1) Å and Ir–Hg(1)–Cl(1) = 172.1(2)°). The [HgCl$_3$]$^-$ anion is linked by Hg(2) to the Cl(1) atom of the cation (Hg(2)...Cl(1) 2.914(6) Å) and through Cl(3) to the Hg(1) atom of a neighboring symmetry-related cation with Hg(1)...Cl(3) 3.011(5) Å.

Introduction

In previously reported chemistry of the half-sandwich Lewis-base complex (η^5-C_5Me_5)Ir(CO)$_2$, we have described the formation of the silver(I) complex cation [{(η^5-C_5Me_5)(CO)$_2$Ir}$_2$Ag]$^+$ and its X-ray structure [1]. In a continuation of our study of the interesting coordination [1–4] and redox [4,5] properties of (η^5-C_5Me_5)Ir(CO)$_2$, we now describe the products of its reactions with the simple dihalides of the zinc group.

Experimental

Compounds were prepared and handled under dry nitrogen. Infrared spectra were obtained for solutions in CaF_2 cells on a Bomem Michelson 120 FTIR instrument. ^{1}H NMR spectra were obtained on a Bruker 100-SY instrument at 100 MHz or on a Bruker WM-400 instrument at 400 MHz. Fast-atom bombardment

---

Correspondence to: Dr. D. Sutton.

mass spectra (FABMS) were obtained on a Hewlett–Packard 5985 GCMS instrument equipped with a Phrasor Scientific Inc. FAB probe (xenon source) and utilized samples dispersed or dissolved in *m*-nitrobenzyl alcohol.

Preparation of complexes

(η^5-C_5Me_5)(CO)$_2$IrZnCl$_2$ (1). A solution of (η^5-C_5Me_5)Ir(CO)$_2$ (15 mg, 3.9×10^{-2} mmol) in diethyl ether (2 mL) was added dropwise with stirring to an excess of anhydrous $ZnCl_2$ in diethyl ether (2 mL). The product precipitated quantitatively as an orange solid that was washed with diethyl ether and dried in a vacuum.

(η^5-C_5Me_5)(CO)$_2$IrCdCl$_2$ (2). A solution of (η^5-C_5Me_5)Ir(CO)$_2$ (32 mg, 8.4×10^{-2} mmol) in ethanol (3 mL) was added dropwise to a solution of excess anhydrous $CdCl_2$ in ethanol (2 mL). The product precipitated quantitatively as a yellow solid that was washed with ethanol and dried in a vacuum.

[(η^5-C_5Me_5)(CO)$_2$IrHgCl][HgCl$_3$] (3b.) A solution of (η^5-C_5Me_5)Ir(CO)$_2$ (35.5 mg, 1.0×10^{-1} mmol) in acetone (3 mL) was treated with a large excess of a concentrated solution of $HgCl_2$ in acetone. The cream precipitate was washed twice with a small amount of acetone and dried in a vacuum. Yield 60.0 mg (70%). Reactions that employed $HgCl_2$ in equimolar or twice-molar proportions to (η^5-C_5Me_5)Ir(CO)$_2$ produced yellow precipitates that were mixtures of **3b** with a second material that is formulated as the 1:1 complex (η^5-C_5Me_5)(CO)$_2$IrHgCl$_2$ (**3a**). IR ν(CO) for **3a**: 2071, 2031 cm^{-1} (acetone); 2071, 2020 cm^{-1} (KBr).

X-Ray structure determination for 3b

X-Ray data collection. The crystallization of [(η^5-C_5Me_5)Ir(CO)$_2$HgCl][HgCl$_3$] (**3b**) was conducted by the slow diffusion of a large amount of acetone into a saturated CH_3NO_2 solution of the complex. A suitable pale yellow crystal, pre-examined by microscopy, was mounted in a glass capillary with some mother liquid about 2 mm behind it. All data were collected at 23 ± 1°C on an Enraf–Nonius CAD4-F diffractometer with graphite monochromatized Mo-K_α radiation. Initially, an orthorhombic unit cell was indicated and was confirmed by the investigation of selected symmetry related reflections. The accurate unit cell was determined from the setting angles of 25 well-centered reflections, widely spread throughout reciprocal space, in the range $23 \leq 2\theta \leq 40°$. Table 1 lists the pertinent crystal and data collection details.

Intensity data in two different octants, (h k l) and (h k $-l$), were collected with $0 < 2\theta \leq 50°$. The ω–2θ scan mode was used in the data collection. Backgrounds were scanned for 25% of the peak width on either side of the peak scan. An analytical absorption correction was not made because the view of the crystal was partially obscured by some mother liquor. Psi-scans based on three high χ angle reflections ($\chi > 82°$) were used for an empirical absorption correction. The intensities of two standard reflections were measured every 80 min of the acquisition time to assess possible crystal decomposition. No appreciable variation in intensity of these standards was observed over the course of the data collection (RMS deviation from the mean was less than 1.5%), so a five-point smoothing curve based on these standard reflections was used to scale the data. Lorentz and polarization corrections were applied. In the data reduction process, a merging of the data from the two different octants (since these are symmetry equivalent) showed good agreement ($R = 3.2\%$ for all valid data; $R = 2.7\%$ for observed data).

Table 1

Crystallographic and experimental data [a] for the complex $[(\eta^5\text{-}C_5Me_5)(CO)_2IrHgCl][HgCl_3]$ (**3b**)

Formula	$Hg_2Ir_1Cl_4OC_{12}H_{15}$	Scan type	Coupled ω-2θ
Formula weight	911.34	Scan range (°)	$1.00 + 0.35 \tan\theta$
Crystal system	Orthorhombic	Scan speed (°/min)	0.82–5.49°
Space group	$P2_1nb$	2θ limits (°)	$0 \leq 2\theta \leq 50$
a (Å)	10.100(2)	Intensity standards	(4, 1, 4); (3, 1, 7)
b (Å)	12.799(3)	Orientational standards	(5, 0, 1); (3, −6, 0); (2, 1, 8)
c (Å)	15.297(3)		
V (Å^3)	1977.3(7)	h, k, l ranges	0, 11; 0, 15; −18, 18
Z	4	Reflections measured	3690
$D_{calc.}$ (mg/m^{-3})	3.112	Unique reflections	1846
$F(000)$	1631.42	Reflections with $I > 3\sigma(I)$ $I > 3\sigma(I)$	1408
μ (Mo-K_α) (mm^{-1})	22.73		
T (K)	293	No. of variables	130
Crystal dimensions (mm)	0.40×0.30×0.20	R_f [b]	0.025
		R_w [c]	0.033 [d]
λ (Å)	0.71069	Goodness of fit [e]	1.36
Transmission factors	0.413–0.999	Max. Δ/σ (final cycle)	< 0.001
		Residual density (e/Å^3)	1.2(2)

[a] Enraf–Nonius CAD4-F diffractometer, Mo-K_α radiation, graphite monochromator. [b] $R_f = \Sigma(|F_o| - |F_c|)/\Sigma|F_o|$. [c] $R_w = [\Sigma w(|F_o| - |F_c|)^2/\Sigma F_o^2]^{1/2}$. [d] $w = [(\sigma(F))^2 + 0.0003F^2]^{-1}$. [e] GOF = $[\Sigma w(|F_o| - |F_c|)^2/(\text{No. of degrees of freedom})]^{1/2}$.

Of the 1846 unique reflections, 1408 reflections were classed as observed ($I_o \geq 3\sigma(I_o)$) and converted into the relative structure factors and their e.s.d.s.

Structure solution and refinement. The structure was solved in the space group $P2_1nb$ with use of a Patterson map to locate the heavy atoms. Subsequent refinement and difference Fourier syntheses led to the location of all remaining non-hydrogen atoms. Scattering factors for neutral atoms were used in the calculation of the structure factors, including anomalous dispersion terms for all non-hydrogen atoms [6]. Anisotropic thermal motion, based on indications from the electron density difference Fourier maps, was refined for Hg, Ir, Cl and O atoms in the structure to yield physically reasonable values. Some of the hydrogen atoms in the C_5Me_5 methyl groups had been revealed directly by using a low angle difference Fourier map, with a sin θ/λ cutoff value of 0.30 Å^{-1}, phased on all non-hydrogen atoms. The coordinates of the remaining hydrogen atoms were calculated. All hydrogen atoms were input as fixed contributions in the subsequent calculations; their idealized positions were repeatedly calculated after cycles of refinement from the geometries of their attached carbon atoms using a C–H distance of 0.96 Å. Isotropic thermal parameters were assigned to these hydrogen atoms, based on those of their attached carbon atoms.

Full matrix least-squares refinement of 130 parameters for 36 atoms converged to $R = 0.025$ and $R_w = 0.033$, with a maximum shift less than 0.001σ. A weighting scheme based on counting-statistics was used in the final refinement, where the weight w was calculated from $w = [(\sigma(F_o))^2 + 0.0003F_o^2]^{-1}$. In the final difference Fourier map, the highest peak had an electron density 1.2(2) e Å^{-3}, and was located in the cation region at a distance 1.17 Å from the Ir atom.

Table 2

Atomic parameters for $[(\eta^5\text{-}C_5Me_5)(CO)_2IrHgCl][HgCl_3]$ (**3b**) (e.s.d.s refer to the last digit)

	x	*y*	*z*	B_{iso} (Å^{-2})
Hg(1)	0.78550(0)	0.28419(6)	0.20859(5)	2.82
Hg(2)	0.54225(12)	0.57825(7)	0.24940(6)	3.66
Ir	1.01523(10)	0.23421(5)	0.14658(4)	1.96
Cl(1)	0.5856(6)	0.3537(5)	0.2622(5)	4.8
Cl(2)	0.3092(5)	0.5650(6)	0.2500(4)	4.8
Cl(3)	0.6190(6)	0.1354(5)	0.1030(4)	3.8
Cl(4)	0.7207(6)	0.6000(5)	0.1483(4)	4.6
O(11)	1.1349(22)	0.2969(16)	0.3210(12)	6.5
O(12)	0.9602(19)	0.0111(12)	0.2013(13)	5.6
C(11)	1.0878(22)	0.2726(18)	0.2573(14)	3.5(4)
C(12)	0.9750(30)	0.0962(21)	0.1823(16)	4.3(5)
C(1)	0.9975(17)	0.2067(14)	0.0026(12)	2.2(3)
C(2)	0.9502(17)	0.3099(14)	0.0199(12)	2.0(3)
C(3)	1.0561(19)	0.3708(15)	0.0604(11)	2.4(3)
C(4)	1.1750(17)	0.3039(14)	0.0584(12)	2.1(3)
C(5)	1.1358(18)	0.2038(15)	0.0264(13)	2.5(4)
C(6)	0.9201(20)	0.1263(17)	−0.0401(13)	2.8(4)
C(7)	0.8224(22)	0.3591(18)	−0.0045(14)	3.5(4)
C(8)	1.0502(20)	0.4845(15)	0.0764(12)	3.0(4)
C(9)	1.3080(30)	0.3359(18)	0.0843(15)	4.3(5)
C(10)	1.2316(21)	0.1179(18)	0.0121(14)	3.4(4)

All calculations were performed on a MicroVAX-II computer by using the NRC VAX Crystal Structure System [7]. Atomic coordinates are listed in Table 2 and selected bond lengths and interbond angles are presented in Table 3. A full listing of the details of the structure determination including observed and calculated structure amplitudes, anisotropic temperature factors and hydrogen coordinates are available from the authors.

Results and discussion

The formation of adducts between neutral half-sandwich organometallic compounds and zinc group metal halides has been documented previously, but not evidently for a complete family of Zn, Cd and Hg complexes. Adducts of $CpCo(CO)_2$ and $HgCl_2$ were synthesized in 1967 by Kemmitt and co-workers [8] and the crystal structures of the 1 : 1 and 1 : 3 complexes confirmed the presence of direct Co–Hg bonds [9,10]. Kemmitt also investigated adducts of the corresponding rhodium complex $CpRh(CO)_2$ with $HgCl_2$ and found that only the 1 : 1 adduct $Cp(CO)_2RhHgCl_2$ was formed [11]. Adducts of the iridium analogues $CpIr(CO)_2$ or $(\eta^5\text{-}C_5Me_5)Ir(CO)_2$ with zinc group dihalides do not appear to have been reported previously. In related chemistry, direct Co–Hg and Co–Zn bonds have been proposed [12,13] in the products of reaction of $CpRh(PMe_3)_2$ with $HgCl_2$ and $ZnCl_2$. More recently, Co–Hg and Rh–Hg bonds have been formulated in the products of the reaction of mercury halides with the linked cyclopentadienyl cobalt complex $\{Co(CO)_2(\eta^5\text{-}C_5H_4)\}_2CH_2$ and with some cyclopentadienyl rhodium vinylidene complexes [14,15]. Extending beyond the cobalt group, complexes of

$HgCl_2$ have been described with, for example, (arene)$M(CO)_3$ (M = Cr, Mo, W) [16,17], $CpM(CO)_2(PPh_3)$ (M = Mn, Re) [18,19], and $CpM(NO)(CO)(PPh_3)$ (M = Mo, W) [20].

The zinc, cadmium and mercury complexes **1**, **2**, **3a** or **3b** readily form as precipitates when $(\eta^5\text{-}C_5Me_5)Ir(CO)_2$ and the metal dichloride are reacted in the appropriate solvents.

$$(\eta^5\text{-}C_5Me_5)Ir(CO)_2 \xrightarrow{MCl_2\ (M=Zn,\ Cd)} (\eta^5\text{-}C_5Me_5)(CO)_2IrMCl_2$$

(**1**) M = Zn
(**2**) M = Cd

$$(\eta^5\text{-}C_5Me_5)Ir(CO)_2 \xrightarrow{HgCl_2} \underset{(\mathbf{3a})}{(\eta^5\text{-}C_5Me_5)(CO)_2IrHgCl_2} \xrightarrow{HgCl_2}$$

$$\underset{(\mathbf{3b})}{[(\eta^5\text{-}C_5Me_5)(CO)_2IrHgCl][HgCl_3]}$$

For zinc, diethyl ether is suitable since $ZnCl_2$ is soluble but the product is only poorly soluble. By comparison, for cadmium the use of diethyl ether to synthesize **2** was not possible, since $CdCl_2$ is insoluble, but ethanol is not suitable for the synthesis of **1** since the product does not precipitate from this solvent. Furthermore, even after prolonged reaction in this solvent, the IR spectrum indicated only weak absorptions attributable to **1** in solution. This suggests that either the rate of formation of **1** in ethanol is slow or more likely that **1** is largely dissociated into its components at equilibrium in this solvent. Thus, successful syntheses of **1** and **2** are dependent on utilizing the insolubility of the products in the requisite solvent. The 1:2 mercury(II) complex, **3b**, was synthesized by addition of a large excess of $HgCl_2$ in acetone, and while the product precipitated, the IR spectrum of the supernatant indicated both that a considerable amount of **3** remained dissolved and that it was not significantly dissociated into $HgCl_2$ and $(\eta^5\text{-}C_5Me_5)Ir(CO)_2$. The addition of a 1:1 stoichiometric amount of $HgCl_2$ in acetone to $(\eta^5\text{-}C_5Me_5)Ir(CO)_2$ gave a material that exhibited elemental composition and an IR spectrum in KBr and acetone that indicated it to be a mixture of **3b** and a second component that is $(\eta^5\text{-}C_5Me_5)(CO)_2IrHgCl_2$ **3a**. The amount of the second component decreased as the proportion of $HgCl_2$ was increased in the reactions and no conditions could be found to obtain this material alone.

Compounds **1**, **2**, **3a** or **3b** were sufficiently stable in solution in CH_2Cl_2 or acetone such that the room temperature solution IR absorptions for $(\eta^5\text{-}C_5Me_5)Ir(CO)_2$ were undetectable over several minutes. However, crystals deposited by hexane diffusion into a CH_2Cl_2 solution of **1** at −10°C over a few days were found by IR to be not **1** but $(\eta^5\text{-}C_5Me_5)Ir(CO)_2$. The cadmium complex **2** could not be recrystallized owing to its low solubility (*e.g.* in CH_2Cl_2 or ethanol) and similar instability in solution. However, the mercury complex **3b** was successfully recrystallized from $MeNO_2$/acetone and is the most stable with respect to dissociation.

The stoichiometry of the complexes has been established from elemental analysis (see Table 4 for analytical and spectroscopic data). Compounds **1** and **2** are 1:1 complexes, whereas the mercury compound **3b** is a 1:2 complex. The X-ray crystal structure of **3b** reveals an ionic structure $[(\eta^5\text{-}C_5Me_5)(CO)_2\text{-}$

Table 3

Selected bond lengths (Å) and inter-bond angles (°) for $[(\eta^5\text{-}C_5Me_5)(CO)_2IrHgCl][HgCl_3]$ (**3b**)

Bond lengths for cation			
Hg(1)–Ir	2.5870(11)	C(1)–C(2)	1.43(3)
Hg(1)–Cl(1)	2.354(5)	C(2)–C(3)	1.46(3)
Ir–C(11)	1.910(22)	C(3)–C(4)	1.48(3)
Ir–C(12)	1.89(3)	C(4)–C(5)	1.43(3)
Ir–C(1)	2.237(18)	C(1)–C(5)	1.44(3)
Ir–C(2)	2.264(19)	C(1)–C(6)	1.45(3)
Ir–C(3)	2.228(18)	C(2)–C(7)	1.48(3)
Ir–Cl(4)	2.284(18)	C(3)–C(8)	1.48(3)
Ir–C(5)	2.240(19)	C(4)–C(9)	1.46(3)
O(11)–C(11)	1.13(3)	C(5)–C(10)	1.48(3)
O(12)–C(12)	1.14(3)		
Bond lengths for anion			
Hg(2)–Cl(2)	2.360(5)	Hg(2)–Cl(3)	2.496(6)
Hg(2)–Cl(4)	2.391(6)		
Bond angles for cation			
Hg(1)–Ir–C(11)	87.4(7)	C(1)–C(2)–C(3)	109.1(15)
Hg(1)–Ir–C(12)	86.1(8)	C(2)–C(3)–C(4)	106.1(15)
C(11)–Ir–C(12)	93.8(10)	C(3)–C(4)–C(5)	107.6(16)
Hg(1)–Ir–Cp* centroid	119.4	C(1)–C(5)–C(4)	109.3(16)
C(11)–Ir–Cp* centroid	129.6	C(2)–C(1)–C(5)	107.5(16)
C(12)–Ir–Cp* centroid	127.1	Ir–C(1)–C(6)	126.8(13)
Ir–Hg(1)–Cl(1)	172.12(15)	Ir–C(2)–C(7)	130.5(13)
Ir–C(11)–O(11)	177.20(21)	Ir–C(3)–C(8)	131.9(13)
Ir–C(12)–O(12)	174.60(22)	Ir–C(4)–C(9)	126.9(14)
		Ir–C(5)–C(10)	127.3(14)
Bond angles for anion			
Cl(2)–Hg(2)–Cl(3)	109.11(20)	Cl(3)–Hg(2)–Cl(4)	110.49(21)
Cl(2)–Hg(2)–Cl(4)	139.67(22)		
Secondary interaction			
Bond lengths			
Hg(2)–Cl(1)	2.914(6)	Hg(1)–Cl′(3)	3.011(5)
Bond angles			
Ir–Hg(1)–Cl′(3)	98.51(11)	Cl(1)–Hg(2)–Cl(2)	94.50(21)
Cl(1)–Hg(1)–Cl′(3)	86.95(19)	Cl(1)–Hg(2)–Cl(3)	100.45(20)
Hg(1)–Cl(1)–Hg(2)	118.56(23)	Cl(1)–Hg(2)–Cl(4)	92.59(20)
Hg(1)–Cl′(3)–Hg′(2)	82.74(16)		

[a] The symmetry equivalent coordinates of these atoms are x, $0.500+y$, $0.500-z$.

$IrHgCl][HgCl_3]$ and the FABMS of this compound exhibits a corresponding mass pattern for the parent cation. For **1** and **2** no crystallographic structure could be determined, but their FABMS also both exhibit similar cation parents with an isotope intensity pattern identical to the theoretical pattern for $[(\eta^5\text{-}C_5Me_5)(CO)_2IrMCl]^+$ (M = Zn, Cd). This may be an indication of an ionic structure for these 1:1 complexes **1** and **2** also, although we cannot discount the possibility that they are not ionic but molecular complexes $[(\eta^5\text{-}C_5Me_5)(CO)_2IrMCl_2]$ as observed in the structure of $Cp(CO)_2CoHgCl_2$ [9]. As expected, the principal fragmentation is by scission of the Ir–M bond so that the next highest mass fragment observed in the spectrum for **1** and **2** corresponds to the radical ion $[(\eta^5\text{-C}_5\text{Me}_5)\text{Ir(CO)}_2]^+$. Thus, there are no observed fragments such as $\text{P}^+ - 28$ corresponding to CO loss from the metal–metal bonded complex cation. The fragmentation of **3b** is much more complex and there is evidence of chlorine transfer processes occurring, as there is a strong pattern at $m/z = 433$ due to $[(\eta^5\text{-C}_5\text{Me}_5)\text{IrCl}_3]^+$.

The infrared spectra of **1**, **2**, **3a** and **3b** in CH_2Cl_2 exhibit the expected two strong ν(CO) absorptions, which are in each case shifted to higher wavenumber compared with $(\eta^5\text{-C}_5\text{Me}_5)\text{Ir(CO)}_2$ (νCO(CH_2Cl_2) 2009, 1939 cm^{-1}). This indicates that the CO groups remain terminal, and the shift is indicative of a withdrawal of electron density from the iridium atom as is to be expected if the metal–metal bond is viewed to arise by donation of an electron-pair from iridium to the Lewis acceptors MCl_2. The limited solubility of **1**, **2** and **3b** in the solvents employed in the synthesis was indicated by the following ν(CO) IR spectra (cm^{-1}) of the supernatant solutions following reaction: **1**: 2062, 2013 (Et_2O); **2**: 2056, 2006 (EtOH); **3b**: 2098, 2060 (acetone).

The ^{1}H NMR resonance for the methyl groups in **1**, **2** or **3b** is a singlet that is slightly shifted downfield from the value for $(\eta^5\text{-C}_5\text{Me}_5)\text{Ir(CO)}_2$ (δ 2.18 (CDCl_3)).

The crystal structure of **3b** shows that the solid is composed of $[(\eta^5\text{-C}_5\text{Me}_5)(\text{CO})_2\text{IrHgCl}]^+$ and $[\text{HgCl}_3]^-$ ions with an extensive network of weak mercury–chlorine bridging contacts linking the cations and anions. As shown in Fig. 1, the cation displays a three-legged piano stool type structure. The iridium–mercury bond length is 2.5870(11) Å, and lies close to values for other iridium–mercury complexes where covalent metal–metal bonding is involved, for example $\text{IrCl}_2(\text{CO})(\text{PPh}_3)_2(\text{HgCl})$ (2.570(1) Å) and $\text{IrBrCl(CO)(PPh}_3)_2(\text{HgBr})$ (2.578(2) Å) [21] and $\text{Ir(COD)(EtN}_3(p\text{-Tol}))(\text{HgCl})$ (2.626(1) Å) [22].

In some other recent structures in which $(\eta^5\text{-C}_5\text{Me}_5)\text{Ir(CO)}_2$ is covalently bonded to an adjacent metal [1,4,23], it has been noted [1] that the C_5Me_5 centroid

Table 4

Analytical and spectroscopic data for **1**, **2** and **3b**

Complex	Analysis [a]		ν(CO) [b] (cm^{-1})	^{1}H NMR [c] (δ)	FAB-MS [d] (m/z)
	C (%)	H (%)			
$(\eta^5\text{-C}_5\text{Me}_5)(\text{CO})_2\text{IrZnCl}_2$ (**1**)	27.51	3.04	2062s	2.28s	483 [e] $[\text{M}^+ - \text{Cl}]$
	(27.69)	(2.88)	2010s		384 [f]
$(\eta^5\text{-C}_5\text{Me}_5)(\text{CO})_2\text{IrCdCl}_2$ (**2**)	25.64	2.53	2054s [g]	2.31s	531 $[\text{M}^+ - \text{Cl}]$
	(25.42)	(2.65)	2006s [g]		384 [f]
$[(\eta^5\text{-C}_5\text{Me}_5)(\text{CO})_2\text{IrHgCl}]$ $[\text{HgCl}_3]$ (**3b**)	15.77	1.48	2098s [h]	2.31s [i]	621 $[\text{M}^+\text{(cation)}]$ [e]
	15.33	1.42	2060s [h]		433 $[(\text{C}_5\text{Me}_5)\text{IrCl}_3{}^+]$
	(15.55)	(1.62)	2085 [j]		691 $[(\text{C}_5\text{Me}_5)(\text{CO})_2\text{IrHgCl}_3{}^+]$
			2045 [j]		

[a] Theoretical values in parentheses. [b] Solution in CH_2Cl_2; s, strong. [c] Solution in CD_2Cl_2; s, singlet. [d] Fast atom bombardment mass spectrum. [e] ^{193}Ir, ^{64}Zn, ^{35}Cl, ^{202}Hg. [f] $(\text{C}_5\text{Me}_5)^{193}\text{Ir(CO)}_2^+$. [g] Weak overall spectrum owing to poor solubility in CH_2Cl_2. [h] Solution in acetone. [i] Solution in DMSO-d_6. [j] In KBr.

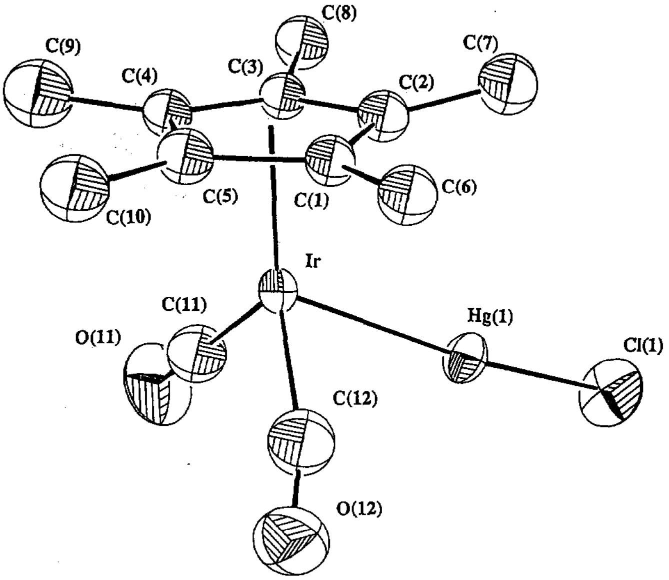

Fig. 1. Perspective view of the cation $[(\eta^5\text{-}C_5Me_5)(CO)_2IrHgCl]^+$ in **3b** with atom labelling. Hydrogen atoms have been omitted.

and CO groups seem to undergo rather little steric re-organization or bending-back from a trigonal planar arrangement around the Ir atom in accommodating the bound metal fragment. The same is true here also, where it is observed that the sum of the interbond angles at iridium formed by the C_5Me_5 centroid, C(11) and C(12) totals 351°, only slightly less than required for a planar arrangement. The C_5Me_5 centroid–Ir–Hg angle (119°) is quite significantly less than the angles subtended at iridium by the C_5Me_5 and either of the carbonyl carbons C(11) or C(12) (129°; 127°).

A view of the structure illustrating the extensive secondary mercury–chlorine interactions that bridge the cations and anions is shown in Fig. 2. The $[HgCl_3]^-$ ion is grossly distorted from the expected regular trigonal planar geometry by its involvement in two long contacts. First, the Hg(2) atom of the anion forms a contact Hg(2) ··· Cl(1) of distance 2.914(6) Å so that Hg(2) becomes pseudo-four-coordinate. Secondly, Cl(3) is connected to the Hg(1)′ atom of the next cation in the chain by a distance Hg(1)′ ··· Cl(3) of 3.011(5) Å. Both of these contacts are significantly shorter than the sum of the van der Waals radii for Hg and Cl (3.30 Å). The other two chlorine atoms of the anion Cl(2) and Cl(4) form no significant contacts, and for these atoms, the Hg–Cl bond lengths are shorter (Hg(2)–Cl(2) = 2.360(5) Å; Hg(2)–Cl(4) = 2.391(6) Å) than the Hg–Cl(3) distance, 2.496(6) Å, as might be expected. One final feature to note is the large angle Cl(2)–Hg(2)–Cl(4) (139.67(22)°) subtended by these two chlorines, compared with the angles subtended by either of these chlorines to the bridging atom Cl(3) (109.1(2)° and 108.5(2)°). One interpretation of this feature and the Hg–Cl bond length variations could be to view the Hg(2)Cl(2)Cl(4) unit as derived from a linear $HgCl_2$ molecule that is not fully complexed by a lone chloride anion Cl(3), and whose mercury atom Hg(2) is making a very unsymmetrical bridge between chlorine Cl(3) and the

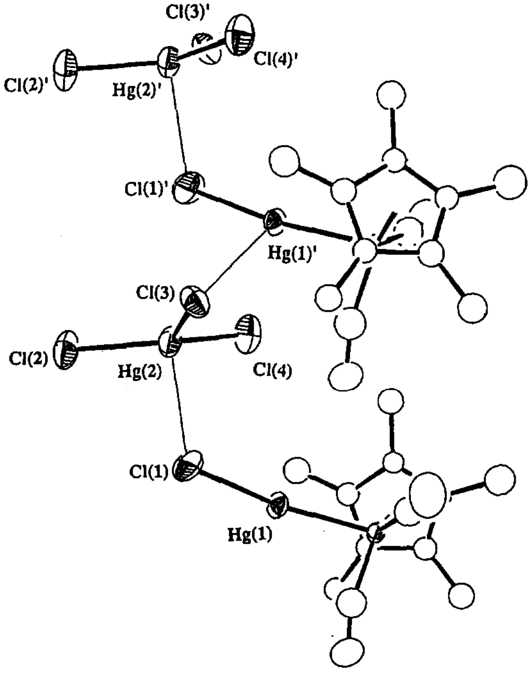

Fig. 2. View of the mercury–chlorine bridging network linking the cations $[(\eta^5\text{-}C_5Me_5)(CO)_2IrHgCl]^+$ and anions $[HgCl_3]^-$ **3b**.

chlorine Cl(1) of the cation. This further illustrates the complex and variable nature of the chlorine bridge structure in compounds with transition-metal bonds to $HgCl_2$ as was first illustrated by Nowell and Russell in connection with the very different arrangements that are adopted for the 1:1 and 1:3 complexes of $HgCl_2$ with $CpCo(CO)_2$ [9,10].

Acknowledgement

This work was supported by NSERC Canada through operating and infrastructure grants to FWBE and DS. We thank Johnson-Matthey Inc. for a generous loan of iridium chloride.

References

1 F.W.B. Einstein, R.H. Jones, X. Zhang and D. Sutton, Can. J. Chem., 67 (1989) 1832.
2 J.M. Zhuang, R.J. Batchelor, F.W.B. Einstein, R.H. Jones, R. Hader and D. Sutton, Organometallics, 9 (1990) 2723.
3 F.W.B. Einstein, X. Yan and D. Sutton, J. Chem. Soc., Chem. Commun., (1990) 1466.
4 F.W.B. Einstein, R.H. Jones, X. Zhang, X. Yan, R. Nagelkerke and D. Sutton, J. Chem. Soc., Chem. Commun., (1989) 1424.
5 F.W.B. Einstein, X. Yan and D. Sutton, Acta Crystallogr., Sect. C, 47 (1991) 1977.
6 International Tables of X-Ray Crystallography, Vol. IV, Tables 2.2B and 2.3.1., Kynoch Press, Birmingham, 1974.
7 E.J. Gabe, Y. LePage, J.-P. Charland, F.L. Lee and P.S. White, J. Appl. Crystallogr., 22 (1989) 384.

8 D.J. Cook, J.L. Dawes and R.D.W. Kemmitt, J. Chem. Soc. A, (1967) 1547; D.J. Cook and R.D.W. Kemmitt, Chem. Ind., (1966) 946.
9 I.W. Nowell and D.R. Russell, J. Chem. Soc., Dalton Trans., (1972) 2393.
10 I.W. Nowell and D.R. Russell, J. Chem. Soc., Dalton Trans., (1972) 2396.
11 J.L. Dawes and R.D.W. Kemmitt, J. Chem. Soc. A, (1968) 1072.
12 K. Dey and H. Werner, J. Organomet. Chem., 137 (1977) C28.
13 K. Dey and H. Werner, Chem. Ber., 112 (1979) 823.
14 M.G. Cox, A.R. Manning and A. McCabe, J. Organomet. Chem., 384 (1990) 217.
15 U. Brekau and H. Werner, Organometallics, 9 (1990) 1067.
16 K. Edgar, B.F.G. Johnson, J. Lewis and S.B. Wild, J. Chem. Soc., A, (1968) 2851.
17 A.M. Ciplus, R.J. Geue and M.R. Snow, J. Chem. Soc., Dalton Trans., (1976) 35.
18 A.G. Ginzburg, G.K.I. Magomedov, A.S. Frenkel, V.N. Setkina and D.N. Kursanov, Izv. Akad. Nauk, SSSR, Ser. Khim., (1978) 2405.
19 A.G. Ginzburg, N.G. Bokyi, A.I. Yanovsky, Yu.T. Struchkov, V.N. Setkina and D.N. Kursanov, J. Organomet. Chem., 136 (1977) 45.
20 A.G. Ginzburg, G.G. Aleksandrov, Yu.T. Struchkov, V.N. Setkina and D.N. Kursanov, J. Organomet. Chem., 199 (1980) 229.
21 P.D. Brotherton, C.L. Raston, A.H. White and S.B. Wild, J. Chem. Soc., Dalton Trans., (1976) 1799.
22 P.I. van Vliet, M. Kokkes, G. van Koten and K. Vrieze, J. Organomet. Chem., 187 (1980) 413.
23 F.W.B. Einstein, R.K. Pomeroy, P. Rushman and A.C. Willis, Organometallics, 4 (1985) 250.